

# M ultifractality in two dimensional random homotopy problem

Raphael Voituriez<sup>1</sup> and Sergei Nechaev<sup>1,2</sup>

<sup>1</sup>UMR 8626, CNRS-Université Paris XI, LPTMS, Bat.100, Université Paris Sud,  
91405 Orsay Cedex, France

<sup>2</sup>L D Landau Institute for Theoretical Physics, 117940, Moscow, Russia

The multifractal properties of distribution of the topological invariants for the trajectories randomly entangled with the nonsymmetric lattices of obstacles are investigated. It is shown explicitly via direct counting for the discrete realization of the model and via conformal methods for the continuous one that the multifractality appears due to breaking the local uniformity of the phase space having exponentially large number of states. The statistical properties of the random walk, such as the drift and the return probability in the topological phase space of the form of locally nonsymmetric tree have been studied by means of renormalization group (RG) technique. The comparison of the analytic RG results to the numerical simulations as well as to the rigorous results of Gehr and Wenz [15] clearly demonstrate the applicability of our approach.

## I. INTRODUCTION

The phenomenon of multifractality consists in a scale dependence of critical exponents. It has been widely discussed in the literature in context of various problems such as, for example, statistics of strange sets [1], diffusion limited aggregation [2], wavelet transforms [3], conformal invariance [4], statistical properties of critical wave function of massless Dirac fermions in a random magnetic field [5-7] and so on.

The aim of our work by no means consists in describing just a new model possessing the multiscaling dependence, while we have in mind the following goal. We would like to show on example of the distribution of entangled random walks in homotopy classes that the phenomenon of multifractality is governed by the local nonuniformity of exponentially growing ("hyperbolic") underlying "target" phase space. In fact, to our knowledge all examples of multifractal behavior in real physical [5-7] and in model [1,8] systems have one common feature: all target phase spaces have noncommutative structure and are locally nonuniform.

We believe that the multiscaling is much more generic physical phenomenon compared to the uniform scaling and appears any time when the phase space of a system has hyperbolic structure with locally perturbed symmetry. Such perturbation could be either regular or random | to our point of view the details of the origin of the nonuniformity play less significant role.

We discuss below the basic features of the multifractality in locally nonuniform regular hyperbolic phase spaces. In particular we show that the multifractal behavior appears in statistical topology when looking at the distribution of entangled (or knotted) random walks in homotopy classes.

The paper is organized as follows. In Section II we consider the 2D random walk in a nonsymmetric array of topological obstacles and investigate the multiscaling properties of the "target" phase space for an ensemble of specific topological invariants, the "primitive paths". The renormalization group computations of the mean length of the primitive path and the return probability in the unentangled topological state of the  $N$  step random walk in the nonsymmetric lattice of obstacles is developed in Section III, while Section IV is devoted to the application of conformal methods for the geometric analysis of the multifractality in regular locally nonuniform hyperbolic spaces.

## II. MULTIFRACTALITY OF TOPOLOGICAL INVARIANTS FOR RANDOM ENTANGLEMENTS IN THE LATTICES OF OBSTACLES

In order to show that the multifractal behavior is not artificial, being attached to very particular models, but is broadly distributed in various physical systems, we re-derive the main features of the multiscaling behavior of statistical systems on example of random entanglement of trajectories in nonsymmetric 2D lattices of obstacles.

The concept of multifractality has been formulated and clearly explained in the paper [1]. Here we recall the basic notions of Renyi spectrum just to make the content of our paper self-contained.

Let  $(C_i)$  be the abstract invariant distribution characterizing the probability of a dynamical system to stay in the basin of attraction of some stable configuration  $C_i$  ( $i = 1, 2, \dots, N$ ). Taking the uniform grid parameterized by the "balls" of size  $l$ , we define the family of fractal dimensions  $D_q$ :

$$D_q = \frac{1}{q} \lim_{l \rightarrow 0} \frac{\ln \sum_{i=1}^{N^l} \mu_i^q (C_i)}{\ln l} \quad (1)$$

As  $q$  is varied, different subsets of  $\mu_i^q$  associated with different values of  $q$  become dominant.

Define the scaling exponent as follows

$$\mu_i^q (C_i) \sim l^q$$

where  $q$  can take different values corresponding to different regions of the measure which become dominant in Eq.(1). In particular, it is natural to suggest that  $\sum_{i=1}^{N^l} \mu_i^q (C_i)$  can be represented

in the form

$$\sum_{i=1}^N q(C_i) = \frac{1}{d^0} \left( \frac{1}{d^0} \right)^{f(0)} \frac{1}{d^0} q$$

where  $(\cdot)$  is the probability to have the value lying in the small "window"  $[0, 0 + \delta]$  and  $f(\cdot)$  is the continuous function which has sense of the fractal dimension of the subset characterized by the value  $\cdot$ .

Supposing  $f'(\cdot) > 0$  one can approximately evaluate the last expression via the saddle-point method. Thus, one gets (see, for example, [1]):

$$\begin{aligned} \frac{d}{d} f(\cdot) &= q \\ \frac{d^2}{d^2} f(\cdot) &< 0 \end{aligned}$$

what together with (1) leads to the following equations

$$\begin{aligned} (q) &= q (q) - f[(q)] \\ (q) &= \frac{d}{dq} (q) \end{aligned} \tag{2}$$

where  $(q) = (q - 1)D_q$ . Hence, the exponents  $(q)$  and  $f[(q)]$  are related via Legendre transform. For further details and more advanced mathematical analysis we could address the reader to [9].

## A . 2D topological systems and their relation to hyperbolic geometry

Topological constraints essentially modify the physical properties of statistical systems consisting of chain-like objects of completely different nature. It should be stressed that topological problems are widely investigated in connection with quantum field and string theories, 2D gravitation, statistics of vortices in superconductors, quantum Hall effect, thermodynamic properties of entangled polymers etc. Modern methods of theoretical physics allow us to describe rather comprehensively the effects of nonabelian statistics on physical behavior for each particular referred system. However, to our opinion, the following question remains still rather obscure: what are the fractal (and as it is shown below, multifractal) properties of the distribution function of topological invariants, characterizing the homotopy state of the statistical system with topological constraints. We investigate this problem in the frameworks of the model "Random Walk in an Array of Obstacles" (RWAO).

The RWAO model can be regarded as physically clear and very representative in age for the system of fluctuating chain-like objects with the full range of nonabelian topological properties. This model is formulated as follows: suppose that  $N$  step random walk of length of the unit

step  $a$  is disposed between the obstacles which form the simple 2D rectangular lattice with the elementary cell of size  $c_x \times c_y$ , where  $c_x$  and  $c_y$  ( $c_y = c_x$ ) are the spacings between neighboring obstacles in horizontal and vertical directions respectively. We assume that the random walk cannot cross ("pass through") any obstacles.

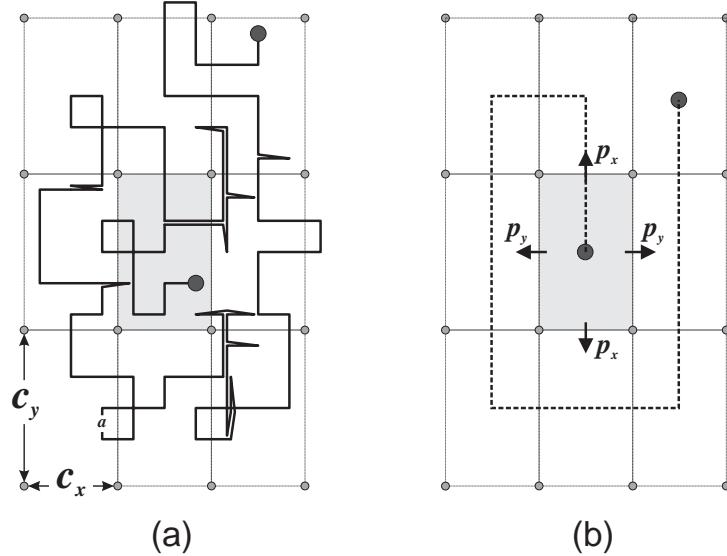


FIG. 1. Random walk in the two-dimensional rectangular lattice of obstacles.

It is convenient to begin with the lattice realization of the RW AO model. In this case the random path can be represented as an  $N$  step random walk in a square lattice with the length of elementary step  $a$  ( $a = c_x = c_y$ ) | see g.1.

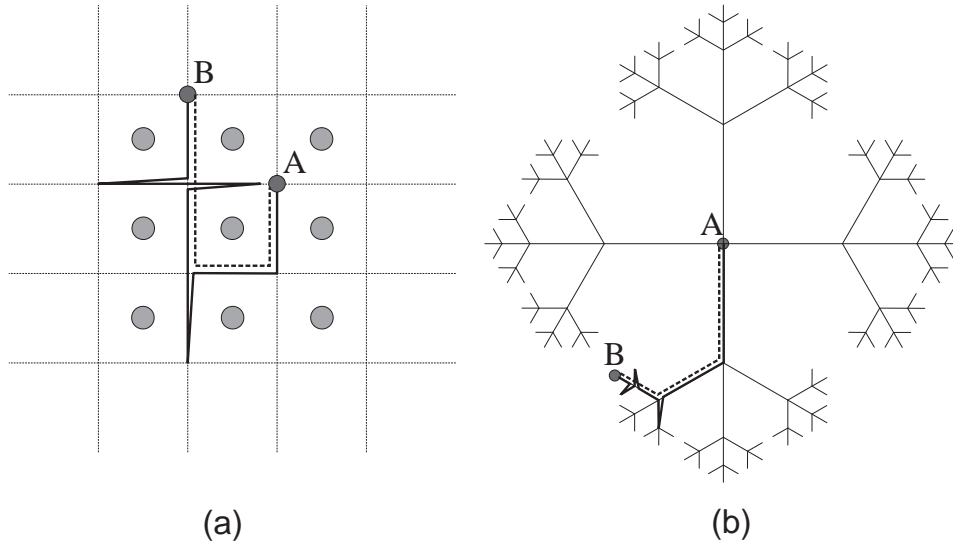


FIG. 2. Random path for  $a = c_x = c_y$ : (a) in the 2D lattice of obstacles; (b) in the covering space (on the Cayley tree).

It had been shown previously (see, for example [10,11]) that for  $a = c_x = c_y$  the lattice random walk in the presence of the regular array of topological constraints produced by uncrossable obstacles (punctures) on the dual lattice  $\mathbb{Z}^2$  is equivalent to the free random walk on the graph of the Cayley tree with the branching number  $z = 4$  (see Fig 2). The outline of the derivation of this result is as follows. Note that the Cayley tree with  $z$  branches (let  $z$  be the even number) plays a role of the universal covering space for the multi-punctured plane and coincides with the graph of the free group  $\mathbb{F}_1$  with the infinite number of generators. At the same time in local basis we have  $\mathbb{F}_1 = \mathbb{Z}^2 = \mathbb{Z}_{z=2}$ , where  $\mathbb{Z}_{z=2}$  is a free group with  $z=2$  generators.

The relation of the Cayley tree with the hyperbolic geometry is discussed in details in Section III, while on the intuitive level such relation could be understood as follows. The Cayley tree can be isometrically embedded into the 3D pseudo-sphere which gives the representation of the non-Euclidean (hyperbolic) plane  $H$  of constant negative curvature. The group  $\mathbb{Z}_{z=2}$  is one of the discrete subgroups of the group of motion of the hyperbolic Poincaré plane  $H = \text{SL}(2; \mathbb{R})/\text{SO}(2)$ .

Returning to the RWAO model, we conclude that each trajectory in the lattice of obstacles can be lifted to the path in the universal covering space i.e. to the path on the branching Cayley tree. The geodesic on the Cayley graph, i.e. the shortest distance along the graph which connects ends of the path plays the role of complete topological invariant for the original trajectory in the lattice of obstacles. For example, the random walk in the lattice of obstacles is closed and completely contractible to the point (i.e. is not entangled with the array of obstacles) if and only if the geodesic length between ends of trajectory on the Cayley graph is equal to zero. Hence, this geodesic length can be regarded as a topological invariant, which preserves all nonabelian features of the problem under consideration.

It is noteworthy to stress two facts concerning our model: (i) The exact configuration of a geodesic is a complete topological invariant, while its length  $k$  is not (except the case  $k = 0$ ); (ii) The length of geodesics has clear geometrical interpretation, having sense of a bar (or "primitive") path which remains after deleting all even times folded parts of random trajectory in the lattice of obstacles. The concept of the "primitive path" was repeatedly used in statistical physics of polymers for successful classification of topological states of chains (like molecules in various topological problems [10{12].

Despite many aspects of statistics of random walks in fixed lattices of obstacles have been well understood (see, for example [13] and references therein), the set of problems dealing with the investigation of fractal properties of the distribution of the topological invariants in the RWAO model are practically out of discussion. Thus we address the next Section to the consideration of fractal and multifractal structure of the measure in the ensemble of primitive paths in the RWAO model in the case  $a = c_y < c_x$ .

B . M ultifractality of the m easure in ensem ble of prim itive paths on the nonsym m etric Cayley tree

The classi cation of different topological states of the  $N$  {step random walk in the rectangular lattice of obstacles in the case  $a = c_y < c_x$  turns to be more difficult and more rich problem than that in the case  $a = c_y = c_x$  considered previously. However after proper rescaling described below, the mapping of the random walk in the rectangular array of obstacles to the random walk on the Cayley tree can be explored again. To proceed we should solve two auxiliary problems. Consider the random walk inside the elementary rectangular cell of the lattice of obstacles. Let us compute:

- (i) The "waiting time", i.e. the average number of steps  $h_{ti}$  which  $t$ {step random walk spends within the rectangle of size  $c_x \times c_y$ ;
- (ii) The ratio of the "escape probabilities"  $p_x$  and  $p_y$  through the corresponding sides  $c_x$  and  $c_y$  for the random walk staying till time  $t$  within the elementary cell.

The desired quantities can be easily computed on the basis of the distribution function  $P(x_0; y_0; x; y; t)$  which has sense of the probability to nd the  $t$ {step random walk with the initial  $(x_0; y_0)$  and nal  $(x; y)$  points within the rectangle of size  $c_x \times c_y$ . The function  $P(x; y; t)$  in continuous approximation ( $a \rightarrow 0; t \rightarrow 1; at = \text{const}$ ) is the solution of the following boundary problem

$$\begin{aligned} \frac{\partial}{\partial t} P(x; y; t) &= \frac{a^2}{4} \frac{\partial^2}{\partial x^2} + \frac{\partial^2}{\partial y^2} P(x; y; t) \\ P(0; y; t) &= P(c_x; y; t) = P(x; 0; t) = P(x; c_y; t) = 0 \\ P(x; y; 0) &= (x_0; y_0) \end{aligned} \quad (3)$$

where  $a$  is the length of the effective step of the random walk and the value  $\frac{a^2}{4}$  has the sense of the diffusion constant.

The solution of Eqs.(3) reads

$$P(x_0; y_0; x; y; t) = \frac{4}{c_x c_y} \frac{x^{\frac{1}{2}}}{m_x = 1} \frac{y^{\frac{1}{2}}}{m_y = 1} e^{-\frac{a^2 t}{4} \left( \frac{m_x^2}{c_x^2} + \frac{m_y^2}{c_y^2} \right)} \sin \frac{m_x x_0}{c_x} \sin \frac{m_y y_0}{c_y} \sin \frac{m_x x}{c_x} \sin \frac{m_y y}{c_y} \quad (4)$$

The "waiting time"  $h_{ti}$  can be written now as follows

$$h_{ti} = \frac{1}{c_x c_y} \int_0^{Z_{c_x}} dx_0 \int_0^{Z_{c_y}} dy_0 \int_0^{Z_{c_x}} dx \int_0^{Z_{c_y}} dy \int_0^{Z_1} dt P(x_0; y_0; x; y; t) \quad (5)$$

while the ratio  $p_x = p_y$  can be computed straightforwardly via the relation:

$$\frac{p_x}{p_y} = \frac{\int_{x_0}^{x_0+c_x} \int_{y_0}^{y_0+c_y} \int_{x_0}^{x_0+c_x} dx P(x_0; y_0; x; y; t) dy P(x_0; y_0; x; y; t) dy_0}{\int_{x_0}^{x_0+c_x} \int_{y_0}^{y_0+c_y} \int_{x_0}^{x_0+c_x} dx P(x_0; y_0; x; y; t) dy P(x_0; y_0; x; y; t) dy_0} \quad (6)$$

In the "ground state dominance" approximation we truncate the sum (4) at  $m_x = m_y = 1$  and arrive at the following approximate expressions:

$$hti = \frac{4^4 c_x^2 c_y^2}{6 a^2 (c_x^2 + c_y^2)}; \quad \frac{p_x}{p_y} = \frac{c_x^2}{c_y^2} \quad (7)$$

In the symmetric case ( $c_x = c_y$ ) Eq.(7) give the values  $hti = \frac{2^7 c^2}{6 a^2}$  and  $p_x = p_y = 1$  as it should be for the square lattice of obstacles.

Now the distribution function of the primitive paths for the random entanglements in the rectangular lattice of obstacles can be obtained via lifting this topological problem to the directed random walk<sup>1</sup> on the 4{branching Cayley tree, where the random walk on the Cayley tree is defined as follows:

(a) The total number of steps  $N$  on the Cayley tree is

$$N = \frac{N}{hti} = \frac{6 N a^2 (c_x^2 + c_y^2)}{4^4 c_x^2 c_y^2}$$

(the value  $hti$  has been computed in (7)).

(b) The distance on the Cayley tree is measured in the "levels"  $k$ , i.e. in the number of steps of directed path between two points on the tree. Each vertex of the Cayley tree has 4 branches; the steps along two of them we take with the Boltzmann weight 1, while the steps along the two remaining ones we take the Boltzmann weight as it is shown in Fig.3. The value of  $\alpha$  is fixed by Eq.(7), so we have

$$\alpha = \frac{p_x}{p_y} = \frac{c_x^2}{c_y^2} \quad (8)$$

The ultrametric structure of the topological phase space, i.e. of the Cayley tree (1), allows us to use the results of the paper [1] for investigating the multicritical properties of the measure of all primitive (directed) paths of  $k$  steps along the graph (1) with nonsymmetric weights 1 and  $\alpha$  (see Fig.3).

---

<sup>1</sup>Recall that by definition the primitive path is the geodesic distance and therefore cannot have two successive opposite steps.

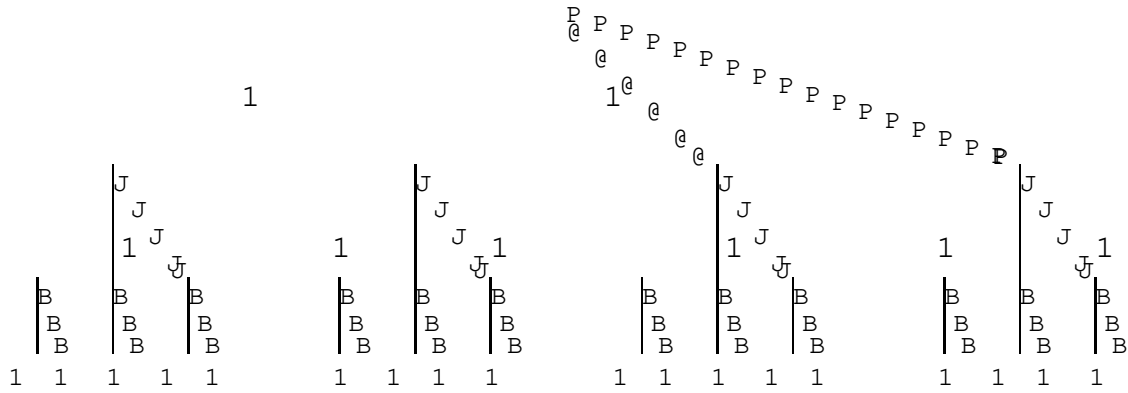


FIG . 3. 4 {branching Cayley tree with di erent transition probabilities along branches.

We construct the partition function  $(\cdot; k)$  which counts properly the weighted number of all  $4^{3^{k-1}}$  different  $k$ -step primitive paths on the graph  $(\cdot)$ .

Define two partition functions  $a_k$  and  $b_k$  of  $k$ -step paths, whose last steps carry the weights 1 and  $J$  correspondingly. These functions satisfy the recursion relations for  $k \geq 1$ :

$$\begin{aligned} & \stackrel{8}{\leftarrow} a_{k+1} = a_k + 2b_k \\ & \therefore b_{k+1} = 2a_k + b_k \end{aligned} \quad (k \geq 1) \quad (9)$$

with the following initial conditions at  $k = 1$ :

$$\begin{aligned} & \stackrel{8}{\leftarrow} a_1 = 2 \\ & \therefore b_1 = 2 \end{aligned} \quad (10)$$

Combining (9) and (10) we arrive at the following 2-step recursion relation for the function  $a_k$ :

$$\begin{aligned} & \stackrel{8}{\leftarrow} a_{k+2} = (1 + \cdot) a_{k+1} + 3a_k \quad (k \geq 1) \\ & \stackrel{8}{\leftarrow} a_1 = 2 \quad (k = 1) \\ & \therefore a_2 = 2 + 4 \quad (k = 2) \end{aligned} \quad (11)$$

which has a solution

$$a_k = \frac{a_2 - a_{k-2}}{1 - 2} \stackrel{k-1}{\underset{1}{\overbrace{+}}} + \frac{a_1 - 1}{1 - 2} \stackrel{k-1}{\underset{2}{\overbrace{+}}} \quad (12)$$

where

$$a_{1,2} = \frac{1}{2} \cdot 1 + \frac{q}{(1 + \cdot)^2 + 12} \quad (13)$$

Taking into account that  $b_k$  is given by the same recursion relation as  $a_k$  but with the initial values  $b_1 = 2$  and  $b_2 = 2^2 + 4$ , we get the following expression for the partition function  $(\cdot; k) = a_k + b_k$ :

$$(\cdot; k) = \frac{2(1 + 4 + 2^2) - 2(1 + \cdot)_2}{1 - 2} + \frac{2(1 + \cdot)_1 - 2(1 + 4 + 2^2)}{1 - 2} \quad (14)$$

The partition function  $(\cdot; k)$  contains all necessary information about the multifractal behavior. Following Eqs.(1){2), we associate the set of stable configurations  $f(C_i)$  with the set of  $N(k) = 4 \cdot 3^{k-1}$  vertices of the Cayley tree on a level  $k$ . Hence, we define

$$\sum_{i=1}^{N(k)} \delta_q(C_i) = \frac{(\cdot; k)}{(\cdot; k)} \quad (15)$$

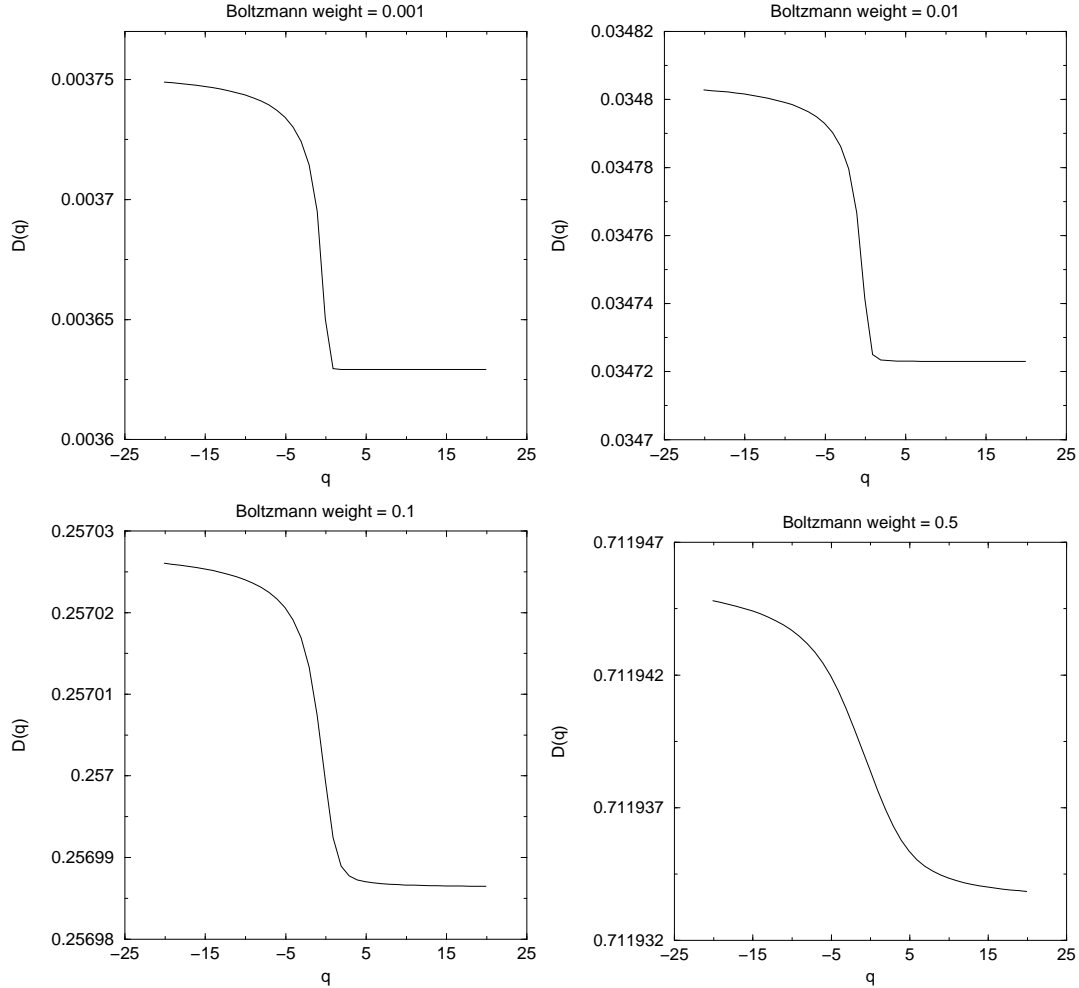


FIG. 4. Dependence  $D_q(q)$  for different values of Boltzmann weight .

Taking into account that the uniform grid has resolution  $l(k) = 1/N(k)$  for  $k = 1$  and using Eq.(1), we arrive at the equation for the function  $D_q(q)$

$$(q) = \lim_{k \rightarrow 1} \frac{\ln (q; k) - q \ln (1; k)}{\ln l(k)} \quad (16)$$

which allows to determine the generalized Hausdorff dimension  $D_q$  via the relation

$$D_q = D_q(q) = (q - 1) \quad (17)$$

The corresponding plots of the function  $D_q(q)$  for different values of Boltzmann weight  $= 0.001; 0.01; 0.1; 0.5$  are shown in Fig.4 (the numerical computations of Eqs.(16)-(17) are carried out for  $k = 100000$ ). The dependencies  $D_q(q)$  clearly demonstrate the multifractal behavior.

### III. RANDOM WALK ON NONSYMMETRIC CAYLEY TREE

#### A. Master equation

Consider the random walk on a 4-branching Cayley tree and investigate the probability distribution  $P(k; N)$  for the  $N$ -step random walk starting at the origin of the tree to have the primitive (shortest) path between ends of  $k$  steps. We call  $k$  for shortness as "the level". The random walk is defined as follows: at each vertex of the Cayley tree the probability of a step along two branches is  $p_x$  and along two other ones is  $p_y$ ;  $p_x$  and  $p_y$  satisfy the conservation condition  $2p_x + 2p_y = 1$  and Eq.(8). So, in terms of  $\alpha$  we have the following expressions for  $p_x$  and  $p_y$ :

$$\begin{aligned} \stackrel{8}{\stackrel{\approx}{\approx}} p_x &= \frac{1}{2(1 + \alpha)} \\ \stackrel{8}{\stackrel{\approx}{\approx}} p_y &= \frac{1}{2(1 + \alpha)} \end{aligned} \quad (18)$$

The symmetric case  $\alpha = 1$  (which gives  $p_x = p_y = 1/4$ ) has already been studied and exact expression for  $P(k; N)$  has been derived [14]. To our knowledge, the solution in the nonsymmetric case is known only for  $k$  fixed in the interval  $0 \leq k \leq N(N-1)$  [15]. We study here the case  $k \leq 1; N \leq 1$ . Breaking the symmetry by taking  $\alpha \neq 1$  one affects strongly the structure of the problem, since now the phase space becomes locally nonuniform: vertices are of two different kinds,  $x$  and  $y$ , depending on whether the step toward the root of the Cayley tree has probability  $p_x$  or  $p_y$ . In order to obtain a master equation for  $P(k; N)$ , we introduce the new variables  $L_x(k; N)$  and  $L_y(k; N)$ , which define the probabilities to be at the

level  $k$  in a vertex  $x$  or  $y$  after  $N$  steps if the walk begins in the root point of the tree. In the same manner we can define recursively the probabilities  $L_{a_1 \dots a_n}(k; N)$ , ( $a_i = fx; yg$ ) to be in such vertex at level  $k$  that the sequence of vertices toward the root is  $a_1 \dots a_n$ . One can see that recursion depends on the total "history" till the root point, what makes the problem nonlocal. The master equation for the distribution function  $P(k; N)$

$$P(k; N+1) = (2p_x + p_y)L_y(k-1; N) + (2p_y + p_x)L_x(k-1; N) + \\ p_y L_y(k+1; N) + p_x L_x(k+1; N) \quad (19)$$

is coupled to the hierarchical set of the functions  $fL_x; L_y; L_{xx}; L_{xy}; L_{yx}; L_{yy}; \dots; L_{a_1 \dots a_n}$  which satisfy the following general recursion relation

$$L_{a_1 \dots a_n}(k; N+1) = (2 \sum_{a_1, a_2} p_{a_1} L_{a_2 \dots a_n}(k-1; N) + \\ p_x L_{x a_1 \dots a_n}(k+1; N) + p_y L_{y a_1 \dots a_n}(k+1; N) \quad (20)$$

where  $a_1 \dots a_n$  cover all sequences of any lengths ( $k$ ) in  $x$  and  $y$ . To close this infinite system at an arbitrary order  $n_0$  we make the following natural assumption: for any  $n > n_0$  we have

$$\frac{L_{a_1 \dots a_n}(k; N)}{P(k; N)} \underset{\substack{k \rightarrow n_0 \\ N \rightarrow n_0}}{\longrightarrow} 1 \quad a_1 \dots a_n \quad (21)$$

with  $a_1 \dots a_n$  constant.

Using the approximation (21) we rewrite (19) { (20) for large  $k$  and  $N$  in terms of the function  $P(k; N)$  and constants  $a_1 \dots a_n$  ( $0 < n < n_0$ ). Taking into account that

$$L_{a_1 \dots a_n x} + L_{a_1 \dots a_n y} = L_{a_1 \dots a_n}$$

we arrive at  $2^{n_0-1}$  independent recursion relations for  $P(k; N)$ , with  $2^{n_0-1}$  independent unknown constants  $a_1 \dots a_{n_0}$ . In order to make the system self-consistent, one and the same functions entering in different equations should be identical, what yields extra  $2^{n_0-2}$  compatibility relations. However the system (19) { (21) is still open. This means that all scales are involved and the evolution of  $L_{a_1 \dots a_n}$  depends on  $L_{a_1 \dots a_{n+1}}$ , the evolution of  $L_{a_1 \dots a_{n+1}}$  depends on  $L_{a_1 \dots a_{n+2}}$  and so on. At each scale we need information about larger scale. This kind of scaling problem naturally suggests using renormalization group approach, which is developed in the next Section.

To begin with the renormalization procedure, we need to estimate the values of the constants  $a_1 \dots a_{n_0}$  for the first (i.e. the smallest) scale. Let us denote

$$\begin{aligned} & 8 \\ & < \quad x = \\ & : \quad y = 1 \end{aligned}$$

and define  $_{xx}$ ;  $_{xy}$ ;  $_{yy}$ ;  $_{yx}$  as follows:

$$\begin{aligned} & \stackrel{8}{\rightsquigarrow} \quad _{xx} = v_x \\ & \rightsquigarrow \quad _{yy} = v_y (1 \quad ) \\ & \rightsquigarrow \quad _{xy} = (1 \quad v_x) \\ & \therefore \quad _{yx} = (1 \quad v_y) (1 \quad ) \end{aligned}$$

Now we set

$$p_{x \ a_1 \dots a_n} + p_{y \ a_1 \dots a_n} = p_x + p_y (1 \quad ) \quad a_1 \dots a_n \quad (22)$$

what means neglecting the correlations between the constants  $a_1 \dots a_n$  and  $a_2 \dots a_n$  on different scales. As is shown in the next Section, the renormalization group approach allows us to get rid of approximation (22).

With (22) one can obtain the following generic master equation

$$P(k; N + 1) = \frac{p_{a_1 \dots a_n}}{a_1 \dots a_n} (2 \quad a_1 \dots a_2) P(k - 1; N) + p_x + (1 \quad ) p_y P(k + 1; N) \quad (23)$$

where  $a_1 \dots a_n$  again cover all possible sequences in  $x$  and  $y$ . We have now  $2^{n_0} - 1$  unknown quantities with  $2^{n_0} - 1$  compatibility relations (23), what makes the system (23) closed. For illustration, we derive the solutions for  $n_0 = 2$ :

$$\begin{aligned} & \stackrel{8}{\rightsquigarrow} P(k; N + 1) = \frac{p_x}{v_x} P(k - 1; N) + p_x + (1 \quad ) p_y P(k + 1; N) \\ & \rightsquigarrow P(k; N + 1) = \frac{2p_x (1 \quad )}{(1 \quad v_x)} P(k - 1; N) + p_x + (1 \quad ) p_y P(k + 1; N) \\ & \rightsquigarrow P(k; N + 1) = \frac{p_y}{v_y} P(k - 1; N) + p_x + (1 \quad ) p_y P(k + 1; N) \\ & \therefore P(k; N + 1) = \frac{2p_y}{(1 \quad ) (1 \quad y)} P(k - 1; N) + p_x + (1 \quad ) p_y P(k + 1; N) \end{aligned} \quad (24)$$

Note that (24) displays clearly  $\mathbb{Z}_2$  symmetry:  $p_x \leftrightarrow p_y$ ;  $v_x \leftrightarrow v_y$ . Compatibility conditions for system (24) read:

$$\frac{p_x}{v_x} = \frac{p_y}{v_y} = \frac{2p_x (1 \quad )}{(1 \quad v_x)} = \frac{2p_y}{(1 \quad ) (1 \quad y)} \quad (25)$$

which finally gives

$$\begin{aligned} & \stackrel{8}{\rightsquigarrow} \quad = \frac{1 \quad 3 \quad + \frac{p}{1 + 14 + \quad ^2}}{2 (1 \quad )} \\ & \rightsquigarrow \quad v_x = \frac{1}{2} \\ & \therefore \quad v_y = \frac{1}{1 + \quad } \end{aligned} \quad (26)$$

As it has been said above, without (22) the system (19)–(20) is open, giving a single equation for the unknown function  $P(k; N)$  depending on the unknown parameter :

$$P(k; N+1) = (2p_x + p_y)(1 - p_y) + (2p_y + p_x)P(k-1; N) + p_y(1 - p_x)P(k+1; N) \quad (27)$$

Eq.(27) describes the 1D diffusion with a drift

$$\frac{hki}{N} - \bar{k} = 2p_y + 2(1 - p_x)p_x$$

and dispersion

$$= \frac{hk}{N} \frac{hki^2}{N} = 1 - 4p_y + (1 - p_x)^2$$

which provides for  $k = 1$  and  $N = 1$  the usual Gaussian distribution with nonzero mean (see [10]). The value of obtained in (26) in the framework of perturbation approach gives a fair estimate for the drift, compared to the numerical simulations, as it is shown in Fig.5.

### B. Real space renormalization

In order to improve the results obtained above, we recover the information lost in the approximation (22) and take into account the interaction between different scales. Namely, we follow the renormalization flow of the parameter  $(l)$  at a scale  $l$  supposing that a new effective step is a composition of  $2^l$  initial lattice steps. Let us define:

the probability  $f(l)$  of going forth (with respect to the location of the root point of the Cayley tree) from a vertex of kind  $a$ ;

the probability  $b(l)$  of going back (towards the root point of the Cayley tree) from a vertex of kind  $a$ ;

the probability  $(l)$  of being at a vertex of kind  $x$ ;

the conditional probability  $w(l)$  to get at a vertex of kind  $a$  starting from a vertex of kind  $a$  under the condition that the step is forth;

the conditional probability  $y(l)$  to get at a vertex of kind  $a$  starting from a vertex of kind  $a$  under the condition that the step was back;

the effective length  $d(l)$  of a composite step.

Then the drift  $\bar{k}(l)$  at a scale  $l$  is given by:

$$\bar{k}(l) = d(l) \stackrel{h}{(l)} f_x(l) \stackrel{i}{b_x(l)} + 1 \stackrel{h}{(l)} f_y(l) \stackrel{i}{b_y(l)} \quad (28)$$

We say that the problems are scale independent if the flow  $\bar{k}(l)$  is invariant under the decimation procedure, i.e. with respect to the renormalization group. We compute the flow counting the appropriate combinations of two steps, depending on the variable considered:

$$\begin{aligned} w_a(l+1) &= 1 \stackrel{h}{w_a(l)} 1 \stackrel{i}{w_a(l)} + w_a^2(l) \\ v_a(l+1) &= 1 \stackrel{h}{v_a(l)} 1 \stackrel{i}{v_a(l)} + v_a^2(l) \\ f_a(l+1) &= \frac{f_a(l) \stackrel{h}{w_a(l)} f_a(l) + 1 \stackrel{i}{w_a(l)} f_a(l)}{c_a(l)} \\ b_a(l+1) &= \frac{b_a(l) \stackrel{h}{v_a(l)} b_a(l) + 1 \stackrel{i}{v_a(l)} b_a(l)}{c_a(l)} \\ d(l+1) &= d(l) \stackrel{h}{(l)} c_x(l) + 1 \stackrel{i}{(l)} c_y(l) \\ (l+1) &= \bar{k}(l) \stackrel{h}{(l)} w_x(l) + 1 \stackrel{i}{(l)} 1 \stackrel{i}{w_y(l)} + \\ &\quad 1 \stackrel{h}{\bar{k}(l)} \stackrel{i}{(l)} v_x(l) + 1 \stackrel{i}{(l)} 1 \stackrel{i}{v_y(l)} \end{aligned} \quad (29)$$

where  $a = x$  when  $a = y$  (and  $a = y$  when  $a = x$ ) and the value  $c_a(l)$  ensures the conservation condition  $f_a(l+1) + b_a(l+1) = 1$  because we do not consider the combinations of two successive steps in opposite directions.

The transformation of in (29) needs some explanations. We consider the drift  $\bar{k}(l)$  as a probability to make a (composite) step forward. The equation for is given by counting the different ways to get at a vertex of kind  $x$ . One can check that  $\bar{k}(l)$  given by (28) remains invariant under such transformation, what is considered as a check of the scale independence (i.e. of renormalizability).

Following the standard procedure, we find the fixed points for the flow of  $(l)$ . First of all we realize that the recursion equations for  $w_a(l)$  and  $v_a(l)$  can be solved independently, providing a continuous set of fixed points:  $w_x^0 = 1 - w_y^0$  and  $v_x^0 = 1 - v_y^0$ . Using the initial conditions (26) for  $v_a(l)$  and deriving straightforwardly the absent initial conditions for  $w_a(l)$ , we get

$$\begin{aligned} v_x(l) &= v_x \\ v_y(l) &= v_y \\ w_x(l) &= w_x = \frac{p_x}{p_x + 2p_y} \\ w_y(l) &= w_y = \frac{p_y}{p_y + 2p_x} \end{aligned} \quad (30)$$

(recall that these values are obtained by taking into account the elementary correlations for two successive steps).

With the initial conditions (30) we find the following renormalized values  $v^0$  and  $w^0$  at the fixed points

$$\begin{aligned} v^0 &= v^0(\ ) = \lim_{l \rightarrow 1} v_x(l) = 1 \quad \lim_{l \rightarrow 1} v_y(l) = \frac{1}{2} \quad (v_x - v_y) \stackrel{l \rightarrow 1}{\rightarrow} f^{(n)}(v_x + v_y) + 1 \\ w^0 &= w^0(\ ) = \lim_{l \rightarrow 1} w_x(l) = 1 \quad \lim_{l \rightarrow 1} w_y(l) = \frac{1}{2} \quad (w_x - w_y) \stackrel{l \rightarrow 1}{\rightarrow} f^{(n)}(w_x + w_y) + 1 \end{aligned} \quad (31)$$

where  $f^{(n)}(x)$  is the  $n$ 's iteration of the function

$$f(x) = x^2 - 2x + 2$$

Hence we obtain successively all renormalized values at the fixed points

$$\begin{aligned} f_a^0 &= 1 \\ b_a^0 &= 0 \\ d^0 &= \overline{k^0} = \frac{v^0 + (1 - v^0)}{1 + (1 - v^0)} \\ \vdots & \quad 0 = \frac{v^0 + w^0}{1 + (1 - v^0)(1 - w^0)} \end{aligned} \quad (32)$$

where the invariance of the drift  $\overline{k}$  is taken into account:

$$\overline{k^0} = \overline{k}(1) = 2p_y^0 + 2p_x(1 - v^0) = \frac{v^0 + (1 - v^0)}{1 + (1 - v^0)}$$

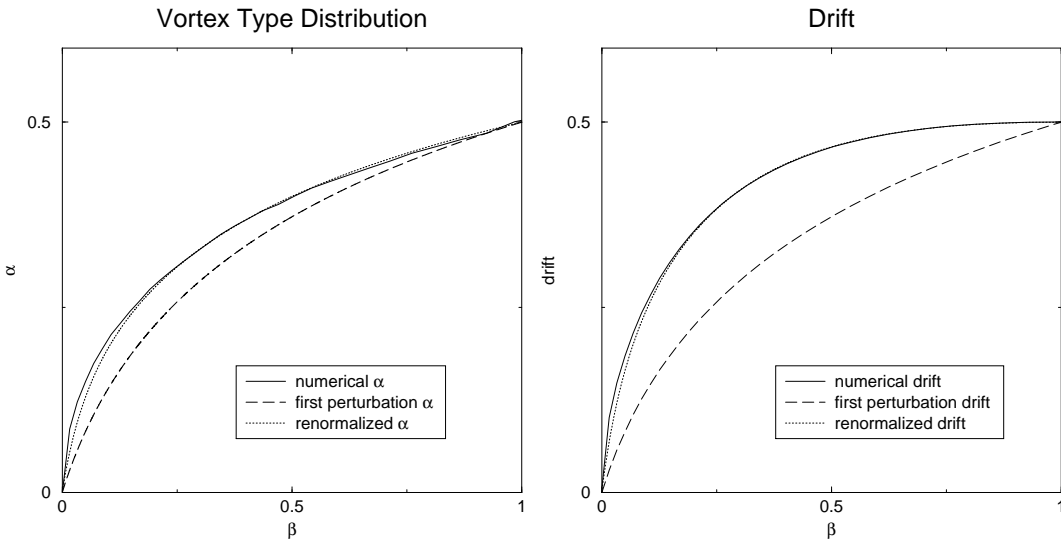


FIG. 5. The values of  $\alpha$  and  $\overline{k}$  compared to renormalized quantities and numerical simulations.

In figure 5 we compare the theoretical results to the numerical simulations. It is worth mentioning the efficiency of renormalization group method, that yields a solution in very good agreement with numerical simulations in a broad interval of values  $k$ .

In addition we compare our results to the exact expression obtained by P. G. de Gennes in [15] for the probability  $P(0; N)$  to return to the origin after  $N$  random steps on the nonsymmetric Cayley tree. This distribution function  $P(0; N)$  reads

$$P(0; N) / N^3 = 2 \quad (33)$$

with

$$z(t) = \min \left( t + \frac{q}{t^2 + 4p_x^2}, t + \frac{q}{t^2 + 4p_y^2} \right) \quad t > 0 \quad (34)$$

Let us assert now without justification that Eq.(27) (which is actually written for  $k=1$  and  $N=1$ ) is valid for any values of  $k$  and  $N$ . The initial conditions for the recursion relation (27) are as follows

$$\begin{aligned} & P(0; N+1) = 2p_x + 2(1-p_x)P(1; N) \\ & P(k; 0) = \delta_{k,0} \end{aligned} \quad (35)$$

One can notice that Eq.(27) completed with the conditions (35) can be viewed as a master equation for a symmetric random walk on a Cayley tree with effective branching  $z$  continuously depending on  $k$ :

$$z(t) = \frac{2}{p_x + (1-p_x)t} \quad (36)$$

Hence, we conclude that our problem becomes equivalent to a symmetric random walk on a  $z(t)$ -branching tree. For  $k=0$  the solution, given in [10] is

$$P(0; N) / \frac{2}{4} \frac{z(t)}{z(t)} \frac{1}{5} N^3 = 2 \frac{q}{t^2 + 4p_x^2} N^3 \quad (37)$$

This provides the same form as the exact solution (33). It has been checked numerically that for  $t \in \mathbb{R}^+$  the discrepancy between (33) and (37) is as follows

$$\frac{1}{(t)} \frac{2}{z(t)} \frac{z(t) - 1}{z(t)} \quad (t) < 0.02$$

Thus, we believe that our self-consistent RG approach to statistics of random walks on nonsymmetric trees can be extended with sufficient accuracy to all values of  $k$ .

#### IV . M U L T I F R A C T A L I T Y A N D L O C A L L Y N O N U N I F O R M C U R V A T U R E O F R I E M A N N S U R F A C E S

We have claimed in Sections I{II that the local nonuniformity of exponentially growing structure of the phase space of some statistical systems is manifested in the multiscaling behavior of corresponding partition functions. In the present Section we are aimed to bring geometric arguments in support of our claim on example of distribution of topological invariants of entangled trajectories with respect to the nonsymmetric lattice of obstacles. The differences of the approach considered in this Section with respect to the one discussed at length of the Section II are as follows:

We consider the continuous model of the random walk topologically entangled with the symmetric and nonsymmetric triangular lattices of obstacles on the plane.

We pursue the goal to construct explicitly the metric structure of the topological phase space via conformal methods and relate directly the nonuniform fractal relief of the topological phase space to the multifractal properties of distribution function in topological invariants for the given model.

Consider the random walks in the regular arrays of topological obstacles on the plane. As in discrete case we can split the distribution function of all  $N$  step paths with fixed positions of end points in different topological classes with respect to the lattice of obstacles. Each topological class we characterize by the topological invariant similar to the "primitive path" defined in the Section II. The conformal methods enable us to investigate the multifractal properties of the distribution function in topological classes for random trajectories in regular lattices of topological obstacles on the complex plane  $z = x + iy$ .

Let us stress that so far explicit expressions are constructed for triangular lattices of obstacles only. That is why we replace the investigation of the rectangular lattices discussed in Sections I{II by the consideration of the triangular ones. Moreover, even for triangular lattices a continuous symmetry parameter (such as  $\gamma = c_x^2 = c_y^2$  in case of rectangular lattices) does not exist and the triangles with angles  $(\alpha = 3; \beta = 3; \gamma = 3)$ ,  $(\alpha = 2; \beta = 4; \gamma = 4)$ ,  $(\alpha = 2; \beta = 6; \gamma = 3)$  are available only such triangles tessellate the whole plane  $z$ . Despite the mentioned restrictions, the study of these cases enables us to figure out the very origin of the multifractality coming from the metric structure of the topological phase space.

Suppose that topological obstacles form a periodic lattice in  $z$  plane. Let the fundamental domain of this lattice be the triangle  $ABC$  with angles either  $(\alpha = 3; \beta = 3; \gamma = 3)$  (symmetric case) or  $(\alpha = 2; \beta = 6; \gamma = 3)$  (most general nonsymmetric case). The conformal mapping  $z(\zeta)$  establishes the one-to-one correspondence between a given fundamental domain  $ABC$  of the lattice of obstacles in  $z$  plane with a zero angled triangle  $A'BC'$  lying in the upper half-plane  $\zeta > 0$  of the

plane  $= +i$  and having corners on real axis  $= 0$ . To avoid possible misunderstandings let us point out that such transform is conformal everywhere except corner (branching) points [ see, for example [16]. Consider now the tessellations of  $z$  plane by means of consecutive reflections of the domain  $ABC$  with respect to its sides and corresponding reflections (inversions) of the domain  $ABC$  in  $\{$  plane. Few first generations are shown in Fig.6. The obtained upper half $\{$  plane  $\text{Im } > 0$  has "lacunary" structure and represents the topological phase space of the trajectories entangled with the lattice of obstacles. The details of such construction as well as the discussion of topological features of the conformal mapping  $z(\cdot)$  in the symmetric case one can find, for example, in [13]. We recall in the meantime the basic properties of the transform  $z(\cdot)$  related to our investigation of the multifractality.

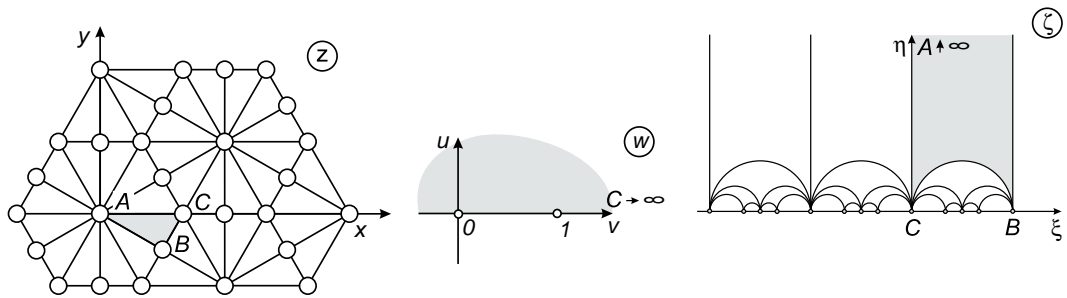


FIG. 6. Conformal mapping of the complex plane  $z$  to the "lacunary" upper half-plane  $\text{Im } > 0$  endowed with a Poincaré metric. The zero{angled triangle  $ABC$  on  $\mathbb{C}$  corresponds to the triangle  $ABC$  with the angles  $(\alpha = 2; \beta = 6; \gamma = 3)$  on  $z$ .

The topological state of some trajectory  $C$  in the lattices of obstacles can be characterized as follows.

Perform the conformal mappings  $z(\cdot)$  (or  $z_{ns}(\cdot)$ ) of the plane  $z$  with symmetric (or nonsymmetric) triangular lattices of obstacles to the upper half-plane  $\text{Im } > 0$  playing role of the topological phase space for a given model.

Connect by nodes the centers of neighboring curvilinear triangles in the upper half-plane  $\text{Im } > 0$  and raise a Cayley tree  $s$  (or  $s_{ns}$ ) isometrically embedded in the Poincaré plane with hyperbolic metric associated with the conformal transforms  $z_s(\cdot)$  (or  $z_{ns}(\cdot)$ ).

Find the image of the path  $C$  in the "covering space"  $\text{Im } > 0$  and define the shortest (primitive) path connecting the centers of the curvilinear triangles where the ends of the path  $C$  are located. The configuration of this primitive path projected to the Cayley tree  $s$  (or  $s_{ns}$ ) plays a role of topological invariant for the model under consideration.

The Cayley trees  $s_{ns}$  have the same topological content as the one described in the Section II however the Boltzmann weights  $\omega_1; \omega_2; \omega_3$  associated with passages between neighboring

vertices (see Fig.7) we would extract now directly from the metric properties (i.e. relief) of the topological phase space obtained via conformal mappings  $z_{\text{sns}}(\cdot)$ .

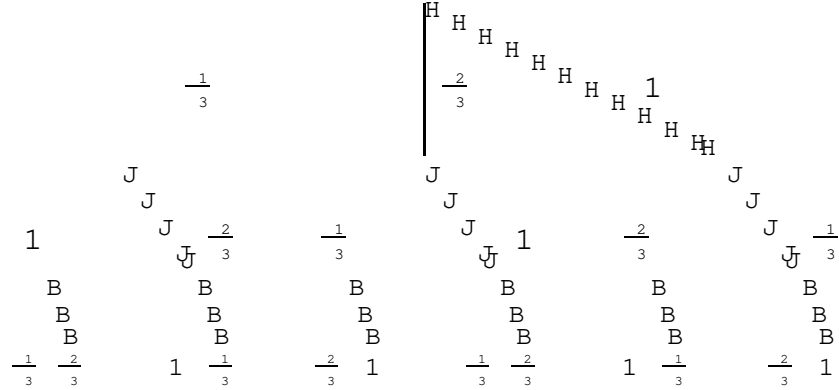


FIG . 7. Non-symmetric 3{branching Cayley tree.

It is well known that the random walk is conformally invariant i.e. the diffusion equation on the plane  $z$  preserves its structure under the conformal transform but the diffusion coefficient becomes to be metric-dependent [17]. Namely, under the conformal transform  $z(\cdot)$  the Laplace operator  $z = \frac{d^2}{dzd\bar{z}}$  is transformed in the following way

$$\frac{d^2}{dzd\bar{z}} = \frac{1}{J^0(\cdot)} \frac{d^2}{d\bar{d}} \quad (38)$$

Before discussing properties of the Jacobians  $J^0(\cdot)$  for the symmetric and non-symmetric transforms, it is more convenient to set up the following geometrical context. The connection between Cayley trees and surfaces of constant negative curvature has already been pointed out [13], mostly through the volume growth considerations. Therefore it becomes more natural to consider the hyperbolic upper half-plane  $\text{Im } z > 0$  endowed with the Poincaré metric of the Riemann surface of the constant negative curvature  $R$  (we here choose arbitrarily  $R = -2$ ):

$$ds^2 = \frac{2}{R^2} (d^2 + d^2) \quad (39)$$

Let us rewrite the Laplace operator (38) in the form

$$\frac{d^2}{dzd\bar{z}} = D(\cdot) \frac{d^2}{d\bar{d}} + \frac{d^2}{d\bar{d}} \quad (40)$$

where the value  $D(\cdot)$   $D(\cdot)$  can be interpreted as the normalized space-dependent diffusion coefficient in Poincaré hyperbolic upper half-plane:

$$D(\cdot) = \frac{1}{\mathcal{P}^0(\cdot)^2} \quad (41)$$

The methods providing the conformal transform  $z_s(\cdot)$  for the symmetric triangle with the angles  $(=3; =3; =3)$  have been discussed in details in [16]. The generalization of these results to the conformal transform  $z_{ns}(\cdot)$  for the nonsymmetric triangle with angles  $(=2; =6; =3)$  is very straightforward. So we expose the final results for the Jacobians of conformal mappings in the symmetric and nonsymmetric cases without derivation:

$$\begin{aligned} \mathcal{P}_s^0(\cdot)^2 &= \frac{1}{B^2 \frac{1}{2}; \frac{1}{3}} \quad {}_0^0(0; e^i) \quad {}^{8=3} \\ \mathcal{P}_{ns}^0(\cdot)^2 &= \frac{2}{B^2 \frac{1}{2}; \frac{1}{3}} \quad {}_0^0(0; e^i) \quad {}^{8=3} \quad {}_2^2(0; e^i) \quad {}^4 \quad {}_3^3(0; e^i) \quad {}^{4=3} \end{aligned} \quad (42)$$

where  ${}_1^0(j::) = \frac{d}{d} {}_1^0(j::)$  and  ${}_i^0(j::)$  ( $i = 0, \dots, 3$ ) are the standard definitions of Jacobi elliptic functions [18].

Combining (41) and (42) we determine the effective inverse division coefficients in the symmetric ( $D_s^{-1}$ ) and in nonsymmetric ( $D_{ns}^{-1}$ ) cases:

$$\begin{aligned} D_s^{-1}(\cdot) &= {}^2 \mathcal{P}_s^0(\cdot)^2 \\ D_{ns}^{-1}(\cdot) &= {}^2 \mathcal{P}_{ns}^0(\cdot)^2 \end{aligned} \quad (43)$$

The corresponding 3D plots of the reliefs  $D_s^{-1}(\cdot; \cdot)$  and  $D_{ns}^{-1}(\cdot; \cdot)$  are shown in Fig.8.

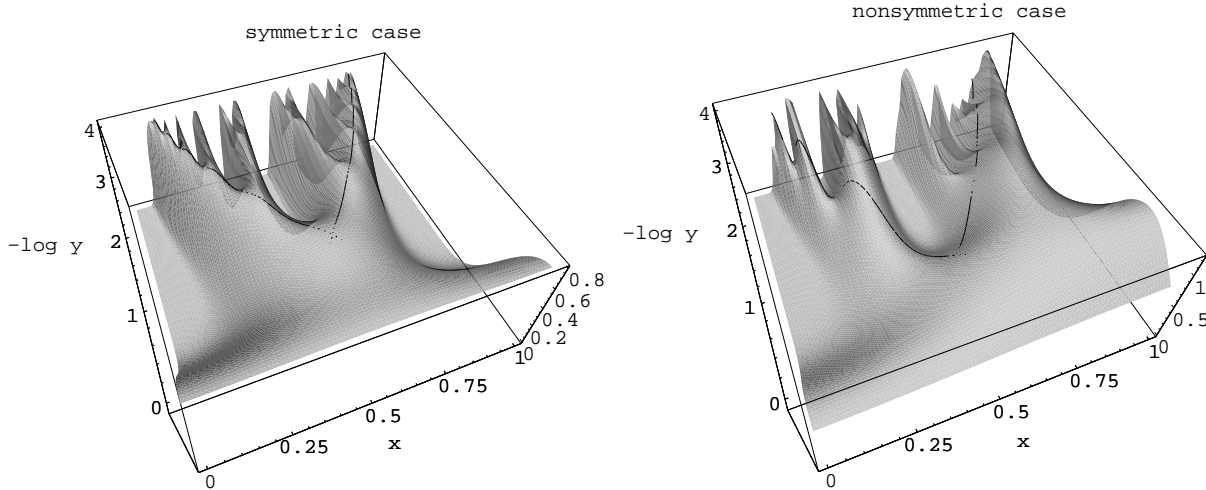


FIG. 8. Profiles of the surfaces  $D_s^{-1}(\cdot; \cdot)$  and  $D_{ns}^{-1}(\cdot; \cdot)$  where  $x; -\log y$ . First generation of horocycles are shown by the lines.

The functions  $D_s^{-1}(\cdot)$  and  $D_{ns}^{-1}(\cdot)$  are considered as quantitative indicators of the topological structure of the phase spaces, and the Cayley trees can be isometrically embedded in such spaces. It can be shown that the images of the centers of triangles of the symmetric lattice in  $\mathbb{Z}^2$  plane corresponds to the local maximum of the surface  $D_s^{-1}(\cdot)$  in  $\mathbb{Z}^2$  plane.

Let us define the horocycles which correspond to repeating sequences of weights in Fig.7 with minimal periods. There are only three such sequences:  $1\ 2\ 1\ 2\ \dots$ ,  $1\ 3\ 1\ 3\ \dots$  and  $2\ 3\ 2\ 3\ \dots$ . The horocycles are images (analytically known) of some circles of the  $\mathbb{Z}^2$  plane. The concept of horocycles is a convenient tool for the constructive description of the trajectories in  $\mathbb{Z}^2$  plane by the trajectories in the covering space.

The first generation of horocycles (closest to the root point of the Cayley tree) is shown in Fig.8. First of all let us consider the symmetric case. One can check that following horocycles we follow the ridges of the surface  $D_s^{-1}(\cdot, \cdot)$ . It is not a set of exactly parabolic points, since  $D_s^{-1}(\cdot, \cdot)$  displays small fluctuations along those ridges. One can nevertheless define locally the embedded Cayley tree as the proper connected part of the set of points where the gradient of the function  $D_s^{-1}(\cdot, \cdot)$  is minimal along its isoline. This set is one-dimensional everywhere except the subset of degenerated points corresponding to the local maximum of  $D_s^{-1}(\cdot, \cdot)$ . Hence we can parameterize the Cayley tree by arcs of horocycles. To give a quantitative formulation of the local definition of the embedded Cayley tree, we consider the path integral formulation of the problem on the  $\mathbb{Z}^2$  plane. Define the Lagrangian  $L / D_s^{-1}(\cdot, \cdot)^2$  of a free particle moving with the division coefficient  $D_s(\cdot)$  in a space. Following the canonical procedure and minimizing the corresponding action [19], we get the equations of motion in the effective potential  $U = \ln(D_s^{-1})^2$ :

$$\ddot{q}_i = (q_j \partial_j U) \dot{q}_i - \frac{1}{2} q_j q_k \partial_i U \quad (44)$$

where  $q_i = \dots$  and  $q_j = \dots$ . Despite Eq.(44) is nonlinear with a friction term, the trajectory of extremal action tends to follow the ridge of the surface  $D_s(\cdot)$  which links the centers of neighboring triangles.

It is noteworthy that obtaining an analytical support of Cayley graphs is of great importance, since those graphs clearly display ultrametric properties and have evident connection to p-adic surfaces [20]. The detailed study of metric properties of the functions  $D_s^{-1}(\cdot)$  and  $D_{ns}^{-1}(\cdot)$  is left for separate publication.

While the self-similar properties of the Jacobians of conformal mappings appear clearly in Fig.8, one could wonder how the symmetry breaking affects the continuous problem. We can see that if  $D_s^{-1}(\cdot)$  is univalued along the embedded tree,  $D_{ns}^{-1}(\cdot)$  does vary, what makes it locally nonuniform and leads to multifractal behavior. In other words, different paths of same length along the tree have the same weights in the symmetric case, but have different ones in the nonsymmetric case. The probability of a random path  $C$  of length  $L$  can be written in terms of a path integral with a Wiener measure

$$p_C = \frac{z}{D} \exp \left( - \frac{1}{D} \int_0^t \frac{ds}{s(t)} \right); \quad (45)$$

where  $s(t)$  is a parametric representation of the path  $C$ .

The first horocycles in Fig.8 can be parameterized as follows

$$\begin{aligned} z &= \frac{1}{2} \left( \frac{1}{3} \sin \frac{p}{3} \right) \\ s &= \frac{1}{3} (1 - \cos p) \end{aligned} \quad (46)$$

with  $p$  running in the interval  $[0, 2\pi]$ . The condition ensuring the constant velocity  $\frac{ds}{dt}$  along the horocycles gives with (39)

$$\frac{1}{2} \frac{d}{dt} = \text{const}$$

hence

$$(t) = \arctan \frac{1}{t} \quad (47)$$

with proper choice of the time unit. This parameterization is used to check that the embedded tree is truly isometric. Indeed, the horocycles shown in Fig.8 corresponds to a periodic sequence of steps like  $1 \ 2 \ 1 \ 2 \dots$ ,  $1 \ 3 \ 1 \ 3 \dots$  or  $2 \ 3 \ 2 \ 3 \dots$ . It is natural to assert that two steps have Boltzmann weights characterized by corresponding local values of  $D_{ns}^{-1}$ . Therefore the period of the plot shown in Fig.9 is directly linked to the spacing of the embedded tree embedded in the profile  $D_{ns}^{-1}$ .

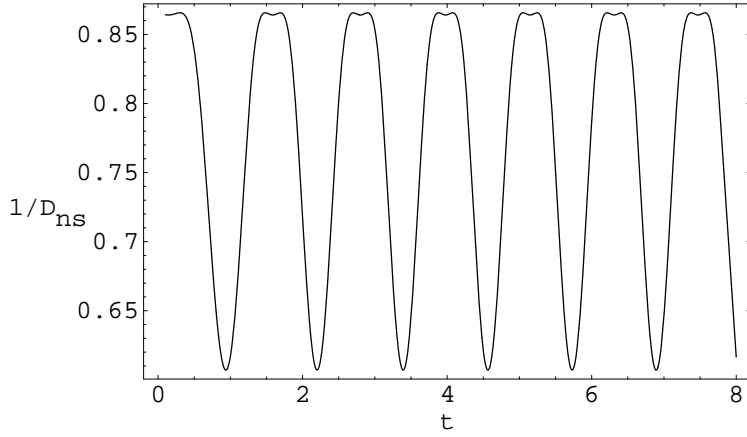


FIG. 9.  $D_{ns}^{-1}$  running along a horocycle at constant velocity. Periodicity shows that the tree is isometric.

Coming back to the probability of different paths covered with constant velocity, one can write:

$$\log p_e / \left[ \frac{dt}{D[s(t)]} \right] \quad (48)$$

The figure 10 shows the value  $\log p_e$  in symmetric and nonsymmetric cases for different paths starting at  $t_1 = 0^+$  and ending at  $t$ . In symmetric case all plots are the same (solid line), whereas in nonsymmetric case they are different: dashed and dotted curves display the corresponding plots for the sequences  $2 \ 3 \ 2 \ 3 \dots$  and  $1 \ 3 \ 1 \ 3 \dots$ .

Following the outline of construction of the fractal dimensions  $D_q$  in the Section II we can describe multifractality in the continuous case by

$$D_q = \frac{1}{q-1} \lim_{L \rightarrow 1} \frac{1}{\ln N(L)} \ln \frac{\int_{Z_L}^{Z_L} D_{fsg} \exp \left( \frac{q}{Z_L} \int_0^{Z_L} D_{ns}^{-1}(s(t)) dt \right) \#_q}{\int_{Z_L}^{Z_L} D_{fsg} \exp \left( \int_0^{Z_L} D_{ns}^{-1}(s(t)) dt \right) \#_q} \quad (49)$$

where  $N(L)$  is the area of the surface covered by the trajectories of length  $L$ . This form contains the behavior obtained in the Section II. Indeed, if instead of the usual Wiener measure one chooses a discrete measure  $d_T$ , which is nonzero only for trajectories along the Cayley tree we recover the following description.

Define the distribution function  $(\frac{1}{3}; \frac{2}{3}; k)$  having sense of number of different paths of  $k$  steps on nonsymmetric branching Cayley tree shown in Fig.7. The values of effective Boltzmann weights  $\frac{1}{3}$  and  $\frac{2}{3}$  are defined in terms of the local heights of the surface  $D_{ns}^{-1}$  along the corresponding branches of the embedded tree. Thus we set

$$\begin{aligned} \frac{1}{3} &= \exp \left[ \int_{t_1}^{Z_L} \frac{dt}{D_{ns}[s_r(t)]} \right] \quad \frac{2}{3} = \exp \left[ \int_{t_2}^{Z_L} \frac{dt}{D_{ns}[s_r(t)]} \right] \quad 1.07; \\ \frac{2}{3} &= \exp \left[ \int_{t_1}^{Z_L} \frac{dt}{D_{ns}[s_l(t)]} \right] \quad \frac{1}{3} = \exp \left[ \int_{t_2}^{Z_L} \frac{dt}{D_{ns}[s_l(t)]} \right] \quad 1.19 \end{aligned} \quad (50)$$

where  $t_1, t_2, t_3$  are adjusted so that  $s_r(t)$  represents a step weighted with  $\frac{1}{3}$  for  $t_1 < t < t_2$  and a step weighted with  $\frac{2}{3}$  for  $t_2 < t < t_3$  for right-hand-side horocycles while  $s_l(t)$  represents a step weighted with  $\frac{2}{3}$  for  $t_1 < t < t_2$  and a step weighted with  $\frac{1}{3}$  for  $t_2 < t < t_3$  for left-hand-side horocycles.

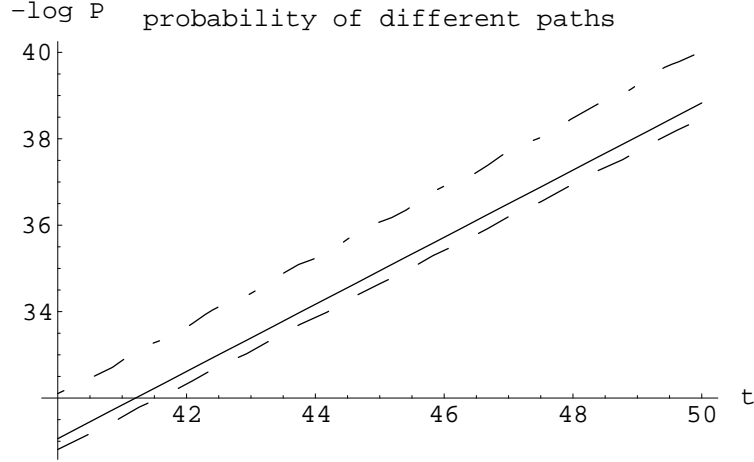


FIG. 10. Probability of different paths along horocycles. Dashed and dot-dashed curves correspond to right-hand and left-hand side horocycles on the non-symmetric surface, while solid line shows both right-hand and left-hand side horocycles on the symmetric surface.

The partition function  $\frac{1}{3}; \frac{2}{3}; k$  can be obtained via straightforward generalization of Eq.(9). It can be written in the form :

$$\frac{1}{3}; \frac{2}{3}; k = A_0 \frac{k-1}{1} + B_0 \frac{k-1}{2} + C_0 \frac{k-1}{3} \quad (k \neq 1) \quad (51)$$

where  $\alpha_1, \alpha_2$  and  $\alpha_3$  are the roots of the cubic equation

$$\frac{1}{3} + \frac{\frac{2}{2}}{\frac{2}{3}} + \frac{\frac{1}{2} \alpha_2}{\frac{2}{3}} = \frac{\frac{1}{2} \alpha_2}{\frac{2}{3}} + \frac{\frac{2}{2}}{\frac{2}{3}} = 0$$

and  $A_0, B_0$  and  $C_0$  are the solutions of the following system of linear equations

$$\begin{aligned} A_0 + B_0 + C_0 &= 1 + \frac{\alpha_1}{3} + \frac{\alpha_2}{3} \\ A_0 \alpha_1 + B_0 \alpha_2 + C_0 \alpha_3 &= 2 \frac{\alpha_1}{3} + 2 \frac{\alpha_2}{3} + 2 \frac{\alpha_1 \alpha_2}{3} \\ \therefore A_0 \frac{\alpha_1^2}{1} + B_0 \frac{\alpha_2^2}{2} + C_0 \frac{\alpha_3^2}{3} &= \frac{\alpha_1}{3} + \frac{\alpha_2}{3} + \frac{\alpha_2^2}{3} + \frac{\alpha_1^2}{3} + 6 \frac{\alpha_1 \alpha_2}{3} + \frac{\alpha_1^2 \alpha_2}{3} + \frac{\alpha_1 \alpha_2^2}{3} \end{aligned}$$

Knowing the distribution function  $\frac{1}{3}; \frac{2}{3}; k$ , Eq.(49) with the discrete measured  $\tau$  reads now (compare to (16)-(17))

$$D_q = \frac{1}{q} \lim_{1/k \rightarrow 1} \frac{\ln \frac{h_{i_q}}{\frac{1}{3}}; \frac{h_{i_q}}{\frac{2}{3}}; k}{\ln (3 - 2^{-1})} \quad (52)$$

The plot of the function  $D_q$  of  $q$  is shown in Fig.11 (the plot is drawn for  $k = 100000$ ).

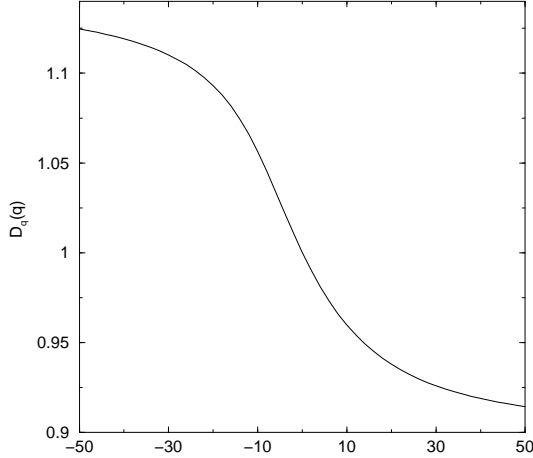


FIG. 11. Multifractality of trajectories on nonsymmetric tree with Boltzmann weights defined by Jacobian of conformal mapping (43).

## V. DISCUSSION

Let us summarize the results obtained in Sections II–IV and pay attention to some related still unsolved problems remaining in the frameworks of our consideration, as well as discuss the applicability of the investigated model in real physical systems.

1. The basic concepts of multifractality have been clearly formulated mainly for abstract systems in the papers [1]. In our work we tried to be as close as possible to these classical formulations, filling in some abstract models of Ref. [1] the new physical content related to topological properties of ensembles of entangled random walks. We believe that the investigation carried out in the present work should explicitly show the sufficient conditions for the physical system to possess the multifractal behavior: (i) the exponentially growing number of the states, i.e. "hyperbolicity", of the phase space, and (ii) breaking the local symmetry of the phase space (while on large scales the phase space could be isotropic).

In the Section II we have considered the topological properties of the discrete model "random walk in the rectangular lattice of obstacles". Generalizing the approach developed earlier (see for example [13] and references therein) we have constructed the topological phase space in form of a nonsymmetric Cayley tree for the trajectories entangled with respect to the rectangular lattice of obstacles. Different effective Boltzmann weights for the passages between nearest neighboring vertices on the Cayley tree have been defined by computing the transition probabilities of the random walk in the nonsymmetric lattice of obstacles with fixed aspect ratio  $\gamma = c_x^2/c_y^2$  (see Eq.(8)). The family of generalized Hausdorff dimensions  $D_q(q)$  for the partition function  $(q; k)$  (where  $k$  is the distance on the Cayley graph which parameterizes the topological state of the trajectory) exhibit the dependence on  $q$  what means that different moments of the partition function  $(q; k)$  scale in different way, i.e. the behavior of  $(q; k)$  is multifractal.

The main topologically probabilistic questions concerning the distribution of random walks in rectangular lattices of obstacles have been considered in the Section III. In particular we have computed the average "degree of entanglement" of the  $N$  step random walk with respect to the immobile rectangular lattice of obstacles and the probability for the  $N$  step random walk to be closed and unentangled with respect to the obstacles. These results we got developing the renormalization group approach on nonsymmetric Cayley tree. The renormalization procedure allowed us to overcome the main difficulty: breaking the symmetry of the local passages on the Cayley tree makes the problem nonlocal such that all scales are involved into the consideration. To verify our procedure we compared the return probability obtained via our RG approach with the exact result of Gérard and Weiss [15] and found very good numerical agreement.

The problem considered in the Section IV correlates with the one discussed at length of the Section II. However we believe that the approach developed in the Section IV could be very important and informative because it explicitly shows that the multifractality is not attached to very particular properties of statistical system under consideration (like random walks in our case) but deals directly with the metric properties of the topological phase space for the nonsymmetric lattice of obstacles. As we have stressed already, some lacks of the conformal approach are due to the fact that the triangular lattices only can be treated easily while the lattices with fundamental domains in form of rectangles demand much evolved computations. Hence, we have considered the complex plane  $z$  tessellated by the lattice of obstacles with the fundamental domain in form of nonsymmetric triangle with angles  $(\pi/2, \pi/3, \pi/6)$ . Performing the conformal mapping  $z_{ns}(\zeta)$  to the universal covering means passing to the topological phase space. We have connected the origin of multifractality with the multi-valley structure of the properly normalized Jacobian  $D_{ns}(\zeta)$  of the nonsymmetric conformal mapping  $z_{ns}(\zeta)$ . The conformal mapping obtained has deep number theoretic properties which we are going to discuss in the forthcoming publication.

2. The "Random Walk in the Array of Obstacles" model can be considered as a basis of a mean-field-like self-consistent approach to the problem of entropy calculation in ensembles of strongly entangled fluctuating polymer chains. Namely, choose the test chain, specify its topological state and assume that the lattice of obstacles models the effect of entanglements with the surrounding chains (the "background"). Changing  $c_x$  and  $c_y$  one can mimic the affine deformation of the background. The investigation of the free energy of the test chain entangled with the deformed media is a very important problem in high-elasticity of polymer rubbers [11].

Neglecting the fluctuations of the background as well as the topological constraints which the test chain produces for itself, we lose some information about the correlations between the test chain and the background. However even in this simplest case we arrive at some nontrivial results concerning the statistics of the test chain caused by topological interactions with the background.

Of course, for the investigation of properties of real systems with topological constraints it is not sufficient to calculate the statistical and topological characteristics of chains in lattices of obstacles, but it is also necessary to be able to adjust any specific physical system to the unique lattice of obstacles. This separate and very complex problem has not been considered in the present work.

The first attempts to go beyond the scope of the mean field approximation of RW AO model and to develop the microscopic approach to statistics of mutually entangled chains like objects have been undertaken recently in [21]. We believe that investigating the multifractality of such systems is worth attending.

#### Acknowledgment

The authors are grateful to A. Comtet for valuable discussions and helpful comments.

- [1] T. Halsey, M. Jensen, L. Kadanoff, I. Procaccia, B. Shraiman, *Phys. Rev. A* 33, 1141 (1986)
- [2] H. Stanley, P. Meakin, *Nature* 335, 405 (1988)
- [3] A. Amendo, G. Grasseau, M. Holschneider, *Phys. Rev. Lett.* 61, 2281 (1988)
- [4] B. Duplantier, *cond-mat/9901008*
- [5] I. Kogan, C. M. Udry, A. Tsvetlik, *Phys. Rev. Lett.* 77, 707 (1996); J. Caux, I. Kogan, A. Tsvetlik, *Nucl. Phys. B* 466, 444 (1996)
- [6] C. Chamon, C. M. Udry, X. Wan, *Phys. Rev. Lett.* 77, 4196 (1996)
- [7] H. Castillo, C. Chamon, E. Fradkin, P. Gódbart, C. M. Udry, *Phys. Rev. B* 56, 10668 (1997)
- [8] B. Derrida, H. Spohn, *J. Stat. Phys.* 51, 817 (1988)
- [9] Ya. Pesin, H. Weiss, *Chaos*, 7, 89 (1997)
- [10] S. Nechaev, A. R. Khokhlov, *Phys. Lett. A* 112, 156 (1985); S. Nechaev, A. N. Semenov, M. K. Koleva, *Physica A*, 140, 506 (1987)
- [11] A. R. Khokhlov, F. F. Ternovskii, *Sov. Phys. JETP*, 63, 728 (1986); A. R. Khokhlov, F. F. Ternovskii, E. A. Zheligovskaya, *Physica A*, 163, 747 (1990)
- [12] E. Helfand, D. Pearson, *J. Chem. Phys.*, 79, 2054 (1983); E. Helfand, M. Rubinstein, *J. Chem. Phys.*, 82, 2477 (1985)

[13] S N echaev, Sov Phys. Uspekhi, 41, 313 (1998); S N echaev, Lect. at Les Houches 1998 Summer School "Topological Aspects of Low Dimensional Systems", cond-mat/9812205

[14] H K esten, Trans Am Math Soc., 92, 336 (1959)

[15] P G erl, W W oess, Prob. Theor. Rel. Fields, 71, 341 (1986)

[16] W K oppenfels, F Stalm an Praxis der Konformen Abbildung (Berlin: Springer, 1959); H K ober, Dictionary of conformal representation (N.Y.: Dover, 1957)

[17] K Ito, H P M cKean, Diffusion Processes and Their Sample Paths (Berlin: Springer, 1965)

[18] M Abramowitz, I Stegun, Handbook on Mathematical Functions (Nat. Bur. Stand., 1964)

[19] R Feynman, A R Hibbs, Quantum Mechanics and Path Integrals (McGraw-Hill, New York 1965)

[20] L B rekke, P F reund, Phys. Rep. 233, 1 (1993)

[21] J Desbois, S N echaev, J Phys. A: Math. Gen., 31, 2767 (1998); A Vershik, S N echaev, R B ikbov, preprint IHES/M/99/45; A Vershik, Russ. Math. Surv., to appear